Hyperfine Interactions 109 (1997) 281–292

Magnetostatic traps for charged and neutral particles

V. Gomer O. Harms, D. Haubrich, H. Schadwinkel, F. Strauch, B. Ueberholz, S. aus der Wiesche and D. Meschede

Institut für Angewandte Physik, Universität Bonn, D-53115 Bonn, Germany

We have constructed magnetostatic traps from permanent magnets for trapping charged and neutral atoms. Two storage experiments are presented: a compact Penning trap for light ions and magnetic trapping of single neutral atoms. The dynamics of cold neutral atoms and their loss mechanisms in a quadrupole magnetostatic trap are discussed.

1. Introduction

Trapping of charged and neutral particles is a powerful experimental tool in many areas of physics. The careful design of homogeneous and inhomogeneous magnetic fields is of critical importance to many such trap configurations. In case of static electromagnetic traps application of strong permanent magnets gives a possibility to study various trapping configurations and physics in such devices in an inexpensive and compact manner.

In principle, arbitrary multipole field configurations with high purity or their combinations can be constructed from strong permanent magnets [1,2]. It is convenient to describe the field in terms of multipole expansion of the potential Φ. For a $2l$-order multipole the potential is given by $\Phi_{lm} \propto r^l Y_{lm}(\theta, \phi)$. Here (r, θ, ϕ) and Y_{lm} denote spherical coordinates and spherical harmonics, respectively. The two practically most important cases are spherical $(m = 0)$ multipoles with rotational symmetry

$$\Phi_l(r, \theta) \propto r^l P_l(\cos\theta), \tag{1}$$

in terms of Legendre polynomials P_l and plane $(m = l)$ or 2-dimensional multipoles without any axial field component

$$\Phi_l(\rho, \phi) \propto \rho^l \cos(m\phi), \tag{2}$$

where (ρ, ϕ) are cylindrical coordinates.

It is well known from Earnshaw's theorem that static potential fields in general and electrostatic fields in particular cannot provide a stable binding force for a charged

particle. A pure magnetic field provides confinement to a cyclotron orbit in the direction transverse to the field lines but not longitudinally.

In a Penning trap [3] the two open ends of the magnetic dipole field can be closed by applying a repulsive electrostatic field near the magnetic poles, which requires an electric quadrupole field. The motion of a charged particle is now confined as long as the magnetic force is larger than the electrostatic force.

A generalization of this principle is obvious: for trapping charged particles one has to superimpose a spherical magnetic l-pole and a spherical electrostatic $2l$-pole. In a magnetic quadrupole field for instance escape of charged particles can be prevented by superposing an electric octupole field. In regions of higher field strength the Penning trap type of motion will qualitatively be preserved. However, even in high field regions the motion is now anharmonic, and near the center it becomes completely irregular. Hence, although this higher order Penning trap is compatible with a trap for paramagnetic neutral atoms, it is not very promising as an experimental tool, because it does not allow for instance to apply proven RF detection schemes.

Static electromagnetic confinement of neutral atoms requires an electric or magnetic dipole force in an inhomogeneous field (higher atomic multipole moments are of academic interest). Unperturbed atoms do not have permanent electric dipole moments because of inversion symmetry, but many atoms have ground or metastable states with magnetic dipole moments that may be used for trapping them. The interaction between an atomic magnetic moment $\vec{\mu}$ and an inhomogeneous magnetic field $\vec{B}$ produces a force given by

$$\vec{F} = -\vec{\nabla}(-\vec{\mu} \cdot \vec{B}). \tag{3}$$

If $\vec{\mu}$ is antiparallel to $\vec{B}$, the atom will be drawn to weaker field regions. The *low-field seekers* will therefore be trapped in a local field minimum. We consider only one minimum in $|\vec{B}|$ so as to obtain maximum localization of the atoms.

For $l > 1$ all spherical multipoles (1) have a zero minimum for the field magnitude at the origin. Hence a spherical quadrupole is the simplest magnetostatic trap for neutral atoms with a magnetic dipole moment, which was employed by Migdal et al. [4] to trap laser-cooled sodium atoms; the next one is a hexapole, which was used for trapping neutrons [5], exhibiting harmonic binding to the center. Plane multipoles (2) provide only lateral confinement and may be used for guiding atoms or closed toroidally for storage rings; furthermore, in combination with spherical multipoles more complicated field configurations can be obtained.

Because of the *zero* minimum in $|\vec{B}|$, the Larmor frequency $\vec{\mu} \cdot \vec{B}/\hbar$ for atoms passing near the origin may be smaller than the orbital frequency, so that the probability of spin-flip transitions to untrapped states may be large [6]. For some experiments it is therefore desirable to have a bias field at the trap center.

It is impossible to construct a magnetic field configuration with a non-zero field-minimum from spherical multipoles only: a combination of an even l (antisymmetrical) multipole with homogeneous (dipole $l = 1$) field shifts only the zero-field point and a combination with an odd l (symmetrical) multipole makes either the radial or the

axial direction unstable. In order to overcome this restriction it is necessary to break cylindrical symmetry.

The simplest variant is the superposition of a magnetic bottle (spherical $l = 1$ and $l = 3$) and a plane quadrupole field ($l = m = 2$). The magnitude of the quadrupole (attractive potential $\propto |\vec{B}| \propto r$) grows with increasing radius faster than the magnetic bottle hexapole (repulsive potential $\propto r^2$) that gives us a trapping configuration for paramagnetic atoms with a *non-zero* minimum point. This is well known as Ioffe–Pritchard [7] or its topological equivalent, baseball trap, that has been successfully used for trapping of hydrogen atoms at MIT [8] and Amsterdam [9] or in experiments with laser-cooled alkali atoms [10]. Ioffe traps of higher order with flatter potential at the center but growing realization difficulties are also possible.

The depth of magnetostatic traps scales as $T = \mu_B \Delta B / k_B \approx 0.67$ K/T with the field difference ΔB between the lowest threshold and the trap minimum and is limited by achievable magnetic fields. Superconducting coils are well adopted for achieving maximum field strength. However, for some experiments, e.g., on strong localization of atoms a small and steep trap rather than a deep and large one is required.

Hence permanent magnets may be competitive or even superior in terms of achievable field gradients at small scales of order of 1 cm [1,2] and offer furthermore compact structures and independence of utilities.

2. Permanent magnets for trapping experiments

Modern rare earth magnetic materials, in the first place SmCo and NdFeB have unique properties. First of all, the remanence B_r of the material is more than 1 T (for NdFeB $B_r \approx 1.1$ T [11]), so large magnetic flux densities can be obtained.

Even more importantly the coercive force H_c (multiplied by the permeability of vacuum) is sufficiently larger than B_r ($H_c \mu_0 \approx 2.07$ T at room temperature). This means that in an assembly of these magnets opposing magnetic fields do not overcome the coercive force and demagnetization effects are negligible.

The relative permeability almost equals 1 ($\mu = 1.08$), that is, one can consider this material as magnetic vacuum and the superposition principle for fields originating from different magnetic pieces is valid. Hence the calculations are reduced to a linear potential problem.

In [1,2] an analytical method for the design of arbitrary multipole field configurations from strong permanent magnet materials has been developed. The idealized continuous rotation of the magnetization needed for maximum possible contribution to a specific multipole at the origin is approximated by a finite number of uniformly magnetized elements.

For a spherical multipole, cylindrical axially and/or radially magnetized rings are used [12]. They are relatively easy to machine, for instance by hot wire erosion, and simple to assemble. In a dipole (homogeneous field) constructed from stacked cylindrical rings a magnetic flux density of the order of the remanence B_r of the

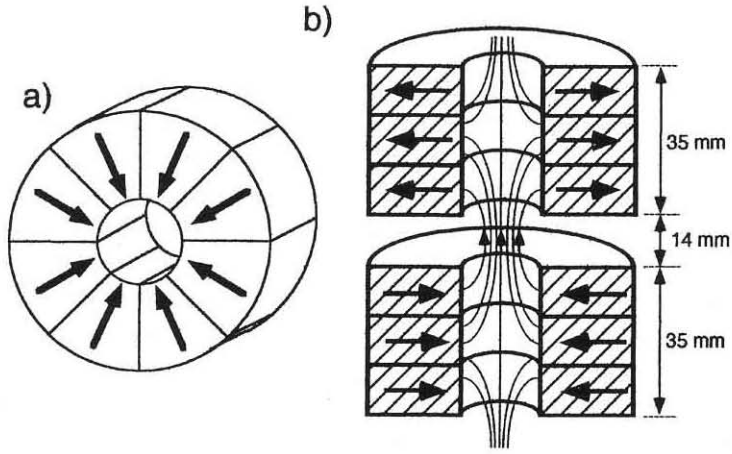

Fig. 1. (a) Magnetic ring assembled from identical uniformly magnetized segments. (b) Magnetic dipole construction from stacked radially magnetized cylindrical rings with flux lines.

magnetic material can be achieved easily. For a quadrupole the magnetic field gradient may overcome 1–2 T/cm.

Useful applications of cylindrical magnetic configurations include Penning traps and quadrupole traps for low field seeking neutral atoms.

A simple version of our Penning trap with permanent magnets is described in [13]. The construction (see fig. 1) gives free access to the trapping region along the symmetry axis and in the radial direction for particle or laser beams, has small size (9 cm length and 5 cm in diameter) and does not need any power supplies (for the electrostatic quadrupole field a battery is enough). The magnetic field of 0.7 T has a homogeneity better than 1% in a volume of 1 cm^3. If necessary the homogeneity can be further improved with shim coils driven at relatively low currents.

The magnet assembly was placed into the vacuum chamber and cooled down to liquid-nitrogen temperature. The base pressure in the cooled system was about 5×10^{-10} Torr. The existence of saddle (quadrupole) points in the magnetic field at the symmetry axis, which in our case are displaced about 2 cm from the trap center, does not cause trouble in loading the trap. An electron gun sending a collimated electron beam along the axis was placed 3 cm above the upper saddle point. An electron current of 0.3 μA was measured at the lower end cap electrode, which is sufficient for the production of ions by ionization of the appropriate residual gas molecules directly in the trapping volume. Various light element ions ($H^{\pm}$, H_2^+, N^+, NH_2^+, NH_3^+) were stored in the trap and storage times up to 3 min were measured. In particular, we have now been able to produce negative hydrogen ions (H^-) by electron impact ionization of NH_3.

The second example is trapping of individual neutral Cs atoms in a quadrupole magnetic trap [14]. A standard magneto-optical trap (MOT) [15] with three orthogonal pairs of counterpropagating $\sigma^+\sigma^-$ laser beams was used to decelerate atoms from the

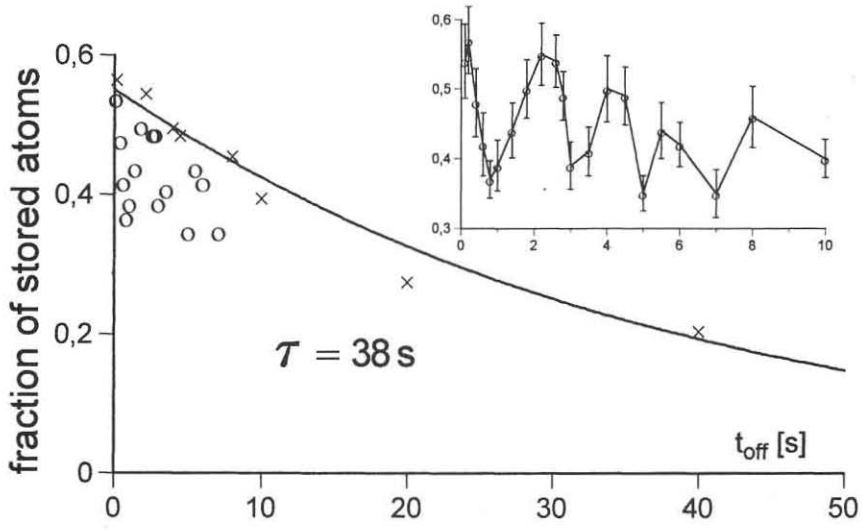

Fig. 2. Magnetic storage of individual atoms. Each data point is the result of more than 100 measurements with single atoms and represents the fraction of atoms detected after the corresponding time with trapping lasers off. The solid line is an exponential fit to the (×) data points yielding a monotonically decreasing function with time constant $\tau = 38$ s. Inset: Apparent oscillating detection probability. Error bars indicate statistical uncertainty.

background gas and load the trap. The magnetic quadrupole field was produced by two opposing stacks of axially magnetized discs with tunable field gradients up to 800 G/cm and a storage volume of a few cm^3.

The fluorescence of the atoms trapped in the MOT was measured with an avalanche photodiode operated in Geiger mode. Well separated discrete steps in the fluorescence signal allow us to monitor the number of trapped atoms. A storage time of 147 s was observed in the MOT at the background pressure of 2×10^{-10} Torr.

At field gradients of 300 G/cm the magnetic force is about 10 times larger than gravity for Cs atoms in the $|F = 3, m_F = -3\rangle$ state, so that purely magnetic trapping of laser-cooled atoms is possible.

Once a single atom was detected in the MOT we switched off the lasers and after a variable time delay then switched on again. Immediately after switch-on we can detect from the fluorescence level whether the atom has survived the dark time or whether it has been lost from the trap.

The result of the measurements is shown on fig. 2. The initial drop of about 50% is a result of the preparation process, which does not select a specific Zeeman sublevel, so that roughly every second atom does not have adequate low field seeking spin orientation and is ejected from the trap. Neglecting the apparent 30% modulation (see below), the following slower decay gives a storage time of 38 s at a pressure of 2×10^{-10} Torr.

The storage time in the magnetic trap is reduced in comparison with the lifetime in the corresponding MOT with identical background pressure. This can be attributed to

the increased relevance of weak collisions with the background gas to atoms trapped in a shallow potential, as we will discuss now.

In order to estimate the lifetime of a single atom in the trap, let us first discuss the losses through non-adiabatic spin-flips [6] near the zero point of the magnetic field. The condition for adiabatic motion (no Majorana transitions) can be written as

$$\omega_{\mathrm{L}} = \frac{\mu_{\mathrm{eff}} B}{\hbar} \gg \left|\frac{\mathrm{d}B}{\mathrm{d}t}\right| \frac{1}{B} = \left|\frac{\mathrm{d}B}{\mathrm{d}r}\right| \frac{v}{B}. \tag{4}$$

For a quadrupole field this means that the displacement from the trap center has to be larger than a critical distance given by

$$r_{\mathrm{crit}} = \left(\frac{\hbar^2}{2m^2 \frac{\partial B}{\partial z}}\right)^{1/3} \tag{5}$$

at all times. At a field gradient of 300 G/cm $r_{\mathrm{crit}} \approx 0.2$ μm for Cs and 5 μm for hydrogen atoms.

In order to estimate the number of trajectories passing through the critical volume near the origin we numerically prepared an ensemble of 1000 atoms with starting positions and velocity orientations distributed randomly at an average energy corresponding to $E/k_{\mathrm{B}} = 100$ μK. Numerical integration of atomic orbits for 10 s has shown that less than 1% have reached displacements from the origin smaller than 50 μm and none of them less than 10 μm. At least for this temperature losses through Majorana spin-flips are statistically irrelevant.

3. Small angle scattering

The storage time in a MOT is known to be limited by collisions with the room temperature ambient gas. In order to remove an atom from such a trap it is necessary to transfer enough energy to leave the trap. The trap depth of our MOT can be estimated to be of the order of 46 mK as determined from the corresponding capture velocity.

Although the depth of a magnetic trap is limited by the maximum magnetic field, in our measurements the effective potential depth is determined by the size of the detection volume (the region irradiated by the laser beams). An atom ejected from the trap center into an orbit with a size larger than the detection volume does not fluoresce and is interpreted as being lost. With 1.5 mm laser beam radius and a magnetic field gradient of 258 G/cm trap depths of 0.4–1.3 mK are obtained, depending on the m_F substate. The kinetic energy of the trapped atoms is less than 100 μK and hence the trap depth is also an approximate measure for the binding energy.

For collision times which are smaller compared to trap oscillation periods both colliding particles can be regarded as free during the scattering process. In a simple

model one can assume a *van der Waals* interaction potential for isotropic atoms, depending on the separation r only,

$$V(r) = -\frac{C}{r^6}. \tag{6}$$

For small scattering angles θ the energy transfer is

$$\delta E = \theta^2 \frac{m}{M} E_{\text{in}}, \tag{7}$$

where E_{in} is the kinetic energy of the incoming fast atoms, M and m are the mass of the trapped and incoming atom, respectively. The classical differential cross section yields [16]

$$\sigma(\theta) = \text{const} \cdot \theta^{-7/3}. \tag{8}$$

The constant depends on the kinetic energy of the incoming particle and is tabulated for various collision partners in [17]. The total loss cross section

$$\sigma_{\text{tot}} = 2\pi \int_{\theta_{\min}}^{\pi} \sigma(\theta) \sin\theta \, \mathrm{d}\theta \tag{9}$$

is determined by

$$\theta_{\min} = \sqrt{\frac{E_{\text{B}} M}{E_{\text{in}} m}}, \tag{10}$$

which corresponds to the minimum energy transfer required to lift a trapped atom across the potential barrier of the trap, i.e., the binding energy E_{B}. This effective cutoff also removes the well known divergence of this classical total cross section for $\theta_{\min} \to 0$.

Since the composition of the background gas is not known, the calculations for the total cross section are made for He–Cs collisions. For room temperature He atoms and the $m_F = -3$ sublevel we can now estimate $\theta_{\min} \approx 0.01$ and the classical total loss cross section $\sigma_{\text{tot}} \approx 1.5 \times 10^{-14}$ cm^2.

At least some of us found it counterintuitive to apply quantum mechanics to the scattering of thermal atoms. An estimation of the critical angle for quantum scattering θ_{crit} shows that it is necessary, however. This critical angle corresponds to the quantum mechanical uncertainty in the position of the scattering particle during the collision event. The latter can be estimated from the maximum impact parameter $b = \sqrt{\sigma_{\text{tot}}/\pi} \approx 7$ Å and is to be compared to the de Broglie wavelength $\lambda_{\text{D}} \approx 0.7$ Å of thermal helium atoms. The classical considerations are valid if the minimum scattering angle $\theta_{\min} \gg \theta_{\text{crit}} = \lambda_{\text{D}}/4\pi b \approx 0.008$, which is obviously not the case here. Hence, the contribution of the quantum corrections to the total loss cross section cannot be neglected. This result is caused by the enormous sensitivity of the shallow trap to weak collisions. Note that the resolving power of the measurement process can be easily increased by reducing the laser beam diameter.

The corrected differential cross section [18]

$$\sigma(\theta) = \text{const} \cdot \theta^{-7/3} \left[1 - \exp\left\{ -(\theta/\theta_{\text{crit}})^{-7/3} \right\}\right] \tag{11}$$

yields $\sigma_{\mathrm{tot}} = (1.38, 1.43, 1.50) \times 10^{-14}$ cm^2 in the magnetic trap, corresponding to a storage time of (69, 67, 64) s for $m_F = -3, -2, -1$, respectively. The weak influence of the magnetic sublevel on the cross section justifies the use of a single exponential fit. Since multiple collisions, each with energy transfer less than the trap depth, can occur, the calculated storage times have to be interpreted as an upper limit.

4. Classical dynamics in a quadrupole trap

Surprisingly, the probability of recapturing the magnetically trapped atom into the MOT oscillates (inset in fig. 2) with a period of order of 2 s, which is not understood up to now. The loss process is by nature irreversible. The probability of capturing a different atom during the detection procedure was less than 4% and has been substracted from the data. So the observed 30% modulation must be a property of the dynamics of the detection process. A magnetically bound atom can walk beyond the detection volume and, due to small laser misalignments, may actually be ejected from the trap by the trapping laser light instead of being detected. However the observed characteristic time of 2 s is not compatible with typical trap oscillation periods of order of 10 ms. Therefore we have begun to study atomic trajectories in the quadrupole trap in more detail.

There are several other reasons for studying the motion of atoms in a magnetic trap. Knowing their positions and velocities may be important for spectroscopy and cooling of atoms. For instance, in the theory of evaporative cooling [19] the basic assumption is "sufficient ergodicity": that is, the distribution of atoms in phase space is assumed to depend only on their energy. This would be the case in a trap with ergodic single-particle motion. The dynamical problem itself with its asymmetric anharmonic potential does not have an analytical solution and is of common interest. Collisionless motion of neutral atoms in a Ioffe trap was discussed in [20].

We can assume that the atom magnetic moment adiabatically follows the local magnetic field, i.e., the atomic motion does not induce any change in the relative orientation of the effective magnetic moment μ_{eff} and field direction. In this case the effective potential energy is

$$V_{\mathrm{mag}} = \mu_{\mathrm{eff}} |\boldsymbol{B}|. \tag{12}$$

Because of azimuthal symmetry of quadrupole field $\boldsymbol{B} \propto (-x, -y, 2z)$ the z-component of the angular momentum L_z is conserved. Consequently the equations of motion are reduced to a two-dimensional problem in (ρ, z) coordinates with effective potential

$$V_{\mathrm{eff}}(\rho, z) = m\left(\frac{\beta}{2}\sqrt{\rho^2 + 4z^2} + gz\right) + \frac{L_z^2}{2m\rho^2}, \tag{13}$$

where

$$\beta = \frac{\mu_{\mathrm{eff}}}{m}\frac{\partial B}{\partial z} \tag{14}$$

is the maximum magnetic acceleration in such a field. For the sake of clarity we introduce a natural radius ρ_0 and a natural time τ

$$\rho_0 = \left(\frac{2L_z^2}{m\mu_{\text{eff}}\frac{\partial B}{\partial z}}\right)^{1/3} \quad \text{and} \quad \tau = \sqrt{\rho_0/\beta} \tag{15}$$

and the ratio

$$\zeta = g/\beta \tag{16}$$

of magnetic and gravitational acceleration. With these definitions we find the minimum or fixpoint of the potential at

$$(\rho_m, z_m) = \frac{\rho_0}{(1-\zeta^2)^{1/6}}\left(1, -\frac{\zeta/2}{(1-\zeta^2)^{1/2}}\right), \tag{17}$$

which reduces to $(\rho_m, z_m) = \rho_0(1,0)$ for $g/\beta \to 0$ as is the case for increasing field gradients. The fixpoint corresponds just to the simple circular motion around the potential symmetry axis with the radius ρ_0 and revolution period $2\pi\sqrt{2}\tau$.

We can also rewrite for convenience the effective Hamilton function, normalized to the natural energy $E_0 = m\beta\rho_0$, and with normalized coordinates $\tilde{z} = z/\rho_0$, $\tilde{\rho} = \rho/\rho_0$ and time $\tilde{t} = t/\tau$, and immediately leaving out the tilde symbols:

$$H_{\text{eff}}(\rho, z) = \frac{1}{2}(\dot{\rho}^2 + \dot{z}^2) + \frac{1}{2}\sqrt{\rho^2 + 4z^2} + \zeta z + \frac{1}{4\rho^2}. \tag{18}$$

In the next step we expand the effective potential in (ρ, z) coordinates to lowest order in a harmonic series,

$$\frac{1}{m}V_{\text{eff}}(\rho, z) \simeq \frac{1}{2}\omega_\rho^2(\rho - \rho_m)^2 + \frac{1}{2}\omega_z^2(z - z_m)^2 + s(\rho - \rho_m)(z - z_m). \tag{19}$$

The harmonic frequencies are calculated from the curvatures of the potential minimum at (ρ_m, z_m) and expressed with the zero gravity frequency $\omega_0^2 = \beta/2\rho_0$,

$$\begin{aligned}
\omega_\rho^2 &= (3+\zeta^2)(1-\zeta^2)^{2/3}\omega_0^2, \\
\omega_z^2 &= 4(1-\zeta^2)^{2/3}\omega_0^2, \\
s &= 2\zeta(1-\zeta^2)^{2/3}\omega_0^2.
\end{aligned} \tag{20}$$

In the zero gravity limit, $\omega_\rho = \sqrt{3}\omega_0$ and $\omega_z = 2\omega_0$, the two oscillations are uncoupled ($s = 0$). The bilinear structure of the equation (19) calls for a normal mode analysis. New eigenfrequencies $\Omega_{\rho,z}$ are obtained from the secular equation

$$\begin{vmatrix} \Omega^2 - \omega_\rho^2 & -s \\ -s & \Omega^2 - \omega_z^2 \end{vmatrix} = 0, \tag{21}$$

yielding (see fig. 3)

$$\begin{aligned}
\Omega_\rho^2 &= \frac{1}{2}\omega_0^2(1-\zeta^2)^{2/3}\left\{(7+\zeta^2) - \sqrt{(1-\zeta^2)^2 + 16\zeta^2}\right\}, \\
\Omega_z^2 &= \frac{1}{2}\omega_0^2(1-\zeta^2)^{2/3}\left\{(7+\zeta^2) + \sqrt{(1-\zeta^2)^2 + 16\zeta^2}\right\}.
\end{aligned} \tag{22}$$

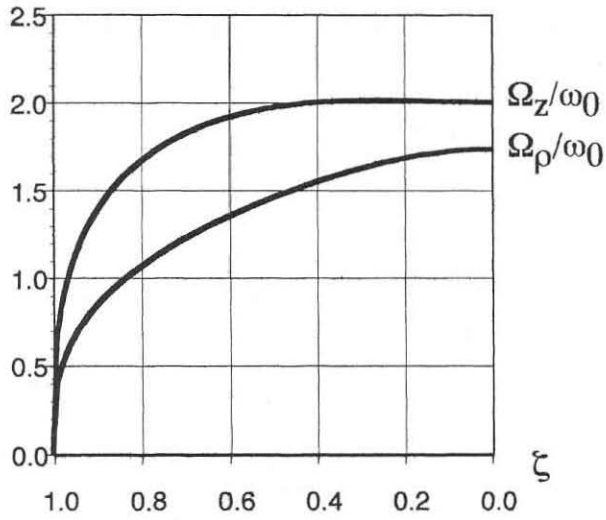

Fig. 3. Eigenfrequencies in a magnetic quadrupole trap as functions of ζ. At $\zeta \to 1$ the trap becomes unstable.

In the first order of perturbation we have two coupled harmonic oscillations with two characteristic frequencies (20). These frequencies scale with the same power of the angular momentum and therefore their ratio is a universal constant for all atoms in the trap (a function of the field gradient only).

We have also numerically integrated classical Hamiltonian equations of motion. From these we have learned that for field gradients of 50–1500 G/cm and energies up to $E/k_B = 1$ mK, i.e., far above typical energies in our experiments, the trajectories are generally regular.

Although the expansion of eq. (20) leading to the simple oscillator description of eq. (22) should be valid only for trajectories slightly deviating from the effective potential minimum it still gives reasonable qualitative agreement at much higher excitation.

As expected from classical nonlinear dynamics with increasing energy chaotic motion sets in first at rational Ω_ρ/Ω_z. For adequate description of unclosed, bounded orbits and to distinguish between chaotic and regular motion Poincare sections were calculated for various magnetic field gradients. For every given ζ we prepared an ensemble of 30 particles of equal energy with positions and velocities distributed randomly. We followed trajectories for up to 1000 points of intersection. The relevant time scale corresponds to several minutes. When the energy approaches some critical value, the stability islands on the Poincare plots break into successively smaller islands showing clearly transition to chaos. In fig. 4 we show the results of our computer simulations.

In conclusion our analysis suggests that trajectories in a quadrupole trap are quasiperiodic for all energies relevant in our experiment.

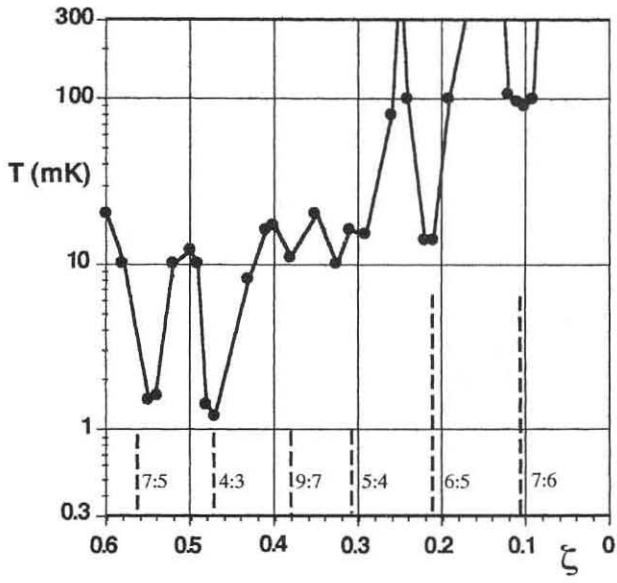

Fig. 4. Threshold energy describing the transition to chaotic motion for various magnetic field gradients. Every point is an averaged result of 30 trajectories simulations for several energies. The stability of the trap does not increase smoothly with growing field gradient ($\zeta \to 0$), but shows nonlinear instability resonances corresponding to rational Ω_1/Ω_2. Usually we have performed our measurements in the region $\zeta \approx 0.15$.

Acknowledgements

This work was funded by the Deutsche Forschungsgemeinschaft. E. Cornell has drawn our attention to ref. [18]. T. Bergeman has provided unpublished material on trajectories in magnetic traps for neutral atoms.

References

[1] K. Halbach, Nucl. Instr. Methods 169 (1980) 1.
[2] V. Frerichs, W.G. Kaenders and D. Meschede, Appl. Phys. A 55 (1992) 242.
[3] L.S. Brown and G. Gabrielse, Rev. Mod. Phys. 58 (1986) 233.
[4] A. Migdal, J. Prodan, W. Phillips, T. Bergeman and H. Metcalf, Phys. Rev. Lett. 54 (1985) 2598.
[5] K.-J. Kugler, W. Paul and U. Trinks, Phys. Lett. 72 B (1978) 422.
[6] E. Majorana, Nuovo Cimento 9 (1932) 43.
[7] Y.V. Gott, M.S. Ioffe and V.G. Tel'kovskii, Nucl. Fusion, 1962 Suppl., Pt. 3 (1962) 1045; D.E. Pritchard, Phys. Rev. Lett. 51 (1983) 1336.
[8] C.L. Cesar et al., Phys. Rev. Lett. 77 (1996) 255.
[9] J.T.M. Walraven, Hyp. Interact. 76 (1993) 205.
[10] V.S. Bagnato, G.P. Lafyatis, A.-G. Martin, E.L. Raab, R.N. Ahmad-Bitar and D.E. Pritchard, Phys. Rev. Lett. 58(21) (1987) 2194; J.J. Tollett, C.C. Bradley, C.A. Sackett and R.G. Hulet, Phys. Rev. A 51(1) (1995) R22.

[11] Magnetfabrik Schramberg GmbH, Max-Planck Str. 15, Postfach 501, D-78713 Schramberg-Sulgen (Material G3-3i).
[12] W.G. Kaenders, V. Frerichs, F. Schröder and D. Meschede, Hyp. Interact. 76 (1993) 221.
[13] V. Gomer, H. Strauss and D. Meschede, Appl. Phys. B 60 (1995) 89.
[14] D. Haubrich, H. Schadwinkel, F. Strauch, B. Ueberholz, R. Wynands and D. Meschede, Europhys. Lett. 34(9) (1996) 663.
[15] E.L. Raab, M. Prentiss, A. Cable, S. Chu and D.E. Pritchard, Phys. Rev. Lett. 59 (1987) 2631.
[16] E.H. Kennard, *Kinetic Theory of Gases* (McGraw-Hill, New York, 1938).
[17] K.T. Tang, J.M. Norbeck and P.R. Certain, J. Chem. Phys. 64(7) (1976) 3063.
[18] R. Helbing and H. Pauly, Z. Phys, 179 (1964) 16;
R.W. Anderson, J. Chem. Phys. 60(7) (1974) 2680;
C.R. Monroe, PhD Thesis (University of Colorado, Bolder, 1992).
[19] O.J. Luiten, M.W. Reynolds and T.W. Walraven, Phys. Rev. A 53 (1996) 381.
[20] E.L. Surkov, J.T.M. Walraven and G.V. Shlyapnikov, Phys. Rev. A 49(6) (1994) 4778.